Microelectronics Reliability 71 (2017) 17–28

Contents lists available at ScienceDirect

Microelectronics Reliability

journal homepage: www.elsevier.com/locate/microrel

# Dynamic pull-in and pull-out analysis of viscoelastic nanoplates under electrostatic and Casimir forces via sinusoidal shear deformation theory

M. Shokravi

*Buein Zahra Technical University, Buein Zahra, Qazvin, Iran*

ARTICLE INFO

*Article history:*
Received 7 November 2016
Received in revised form 7 February 2017
Accepted 7 February 2017
Available online 28 February 2017

*Keywords:*
Nano-switch
Pull-in voltage and time
Pull-out voltage
Viscoelastic nanoplate
Surface effect

ABSTRACT

In the present research, dynamic pull-in and pull-out analysis of viscoelastic nanoplate switch under electrostatic and intermolecular Casimir forces are studied. The Viscoelastic properties of the nanoplate are considered using Kelvin-Voigt model. Sinusoidal shear deformation theory is utilized for mathematical modeling of the structure due to its accuracy of polynomial function than other plate theories. The surface effects are considered based on Gurtin-Murdoch theory to enhance the accuracy of results. Considering size effects based on Eringen's nonlocal theory, motion equations are derived using Hamilton's principle and solved by Galerkin's method. Considering two boundary conditions of clamped in all edges (CCCC) and clamped in two edges and free in tow another edges (CCFF), the influences of various parameters such as small scale effect, surface layer, viscoelastic damping coefficient and applied voltage on the pull-in voltage, pull-in time, pull-in deflection and pull-out voltage are discussed in details. Numerical results indicate that considering small scale effects, the pull-in time and voltage as well as pull-out voltage are increased and decreased, respectively, for CCFF and CCCC boundary conditions. In addition, as the effective gap distance increases, the pull-out voltage tends toward the pull-out voltage. The results of this investigation can be used in control and optimum design of smart nano-electrical devices in advanced applications as smart controller.

© 2017 Elsevier Ltd. All rights reserved.

## 1. Introduction

Recently electrostatically actuated nanoplates because of their simple structures are widely used in many Nano-Electro-Mechanical Systems (NEMS) and Micro-Electro-Mechanical Systems (MEMS) devices, such as nano-sensors, pressure sensors, nano-actuators and etc. [1–3].

Those systems can be defined as smart function with few mechanical components and small voltage levels to work. In general, a nano-switch is composed of two electrodes that one of them is a ground plane and another one is movable electrode which they are separated by a dielectric medium. The movable electrode will be deformed by applying voltage [4]. When this voltage increases to one critical, it makes collapsing the nanoplates that called pull-in instability. The critical voltage, time and deflection related with this instability are named pull-in voltage, pull-in time and pull-in deflection, respectively [5]. They are very important parameters to switching the system. At nano-switch systems; there are some essential phenomena which are not important at macro scales, such as the effect of gap length between two electrodes of a switcher [6].

Lately, pull-in behavior of nano-structures [7–11] is studied by many researchers. Based on the gap between two electrodes, the intermolecular force "Casimir force" becomes important [12–13]. Batra et al. [14] studied the vibrations and pull-in instabilities of micro-electro-mechanical plate incorporating the Casimir force. They derived the reduced-order model for the transverse deflection of micro-plate. Lin and Zhao [15] studied the Casimir effect on the pull-in gap and pull-in voltage of NEMS switches. They also derived dynamic behavior of nano-scale electrostatic actuators. Jia et al. [16] investigated pull-in instability of geometrically nonlinear micro-switches under electrostatic and Casimir forces. They obtained pull-in voltage and pull-in deflection for micro-switches with four different boundary conditions. Their results show large deformation at some geometric configurations can be borne by electro-statically actuated nano-structures [17–20].

Due to the size dependency of the material behaviors, the classical continuum mechanics is not appropriate in the nano-structures [21–24] so, the nonlocal elasticity theory is suggested to investigate the effect of small scale [25–26]. In this regard, Yang et al. [27] proved the small scale effect on the pull-in instability of nano-switches subjected to the electrostatic force created by the applied voltage and intermolecular force. They applied a linear distributed load model to find closed form results for cantilever nano-switch by fixed-fixed boundary conditions. They found that in cantilever nano-switches, an increase in the small scale factor leads to a higher pull-in voltage. Ghorbanpour et al. [28] investigated the nonlinear nonlocal pull-in instability of boron nitride nano-switches considering the van der Waals (vdW) force under

*E-mail addresses:* Maryamshokravi10@gmail.com, Maryamshokravi10@bzte.ac.ir.

http://dx.doi.org/10.1016/j.microrel.2017.02.006
0026-2714/© 2017 Elsevier Ltd. All rights reserved.

direct voltage. They derived the higher-order nonlinear governing equations based on the principle of virtual work. Using the differential quadrature method (DQM), the effects of small-scale parameter, electric potential and external forces on the pull-in phenomenon of the boron nitride nanotubes (BNNTs) are established. In many articles, nanoplates are modeled as viscoelastic plates. Su et al. [29] studied the viscoelastic properties of graphene oxide nano-plate experimentally. Pull-in analysis of electrically actuated viscoelastic micro-beams based on a modified couple stress theory is proposed by Zhang and Fu [30]. They studied on the instantaneous pull-in voltage, durable pull-in electrostatic and vdW forces. Their results show when the effective gap distance increases, the pull-out voltage tends toward the electro-statically pull out voltage.

The surface-to-bulk energy ratio increases in nano-scale problems. On the other hand, surface energy can play a vital function in the pull-in manners of nano-switches. The influence of surface energy on the pull-in instability of electrostatic nano-switches based on geometrically linear deformation was discussed by Maetal [31]. Wang and wang [32] presented a modified continuum model for electrically actuated nano-beams by incorporating surface elasticity. They investigated the effects of the surface energies on the static and dynamic responses, Pull-in voltage and Pull-in time.

After collapsing the structure to the substrate (pull-in instability), the pull-out problem begins. In this state, due to the vdW or Casimir force, a new force which is named stiction exists. However, decreasing the applied voltage, the structure pulls-out from the dielectric when the elastic restoring force of the beam balances with the total of the electrostatic and stiction forces. This maximum value of voltage is the pull-out voltage. In this regards, there are few works in the literature. Basu et al. [33] estimated the stiction force from electrical (current–voltage) measurements on surface micromachined polysilicon cantilever beams. The effects of stiction forces on the pull-out voltage of electrostatically actuated microcantilever beams were theoretically and experimentally investigated by Chakraborty et al. [34]. Recently, Ghorbanpour et al. [28] reported the pull-out voltage for the BNNT switches.

Despite of mentioned researches, dynamic pull-in and pull-out analysis of viscoelastic nanoplate switch via sinusoidal shear deformation theory is a novel topic that cannot be found in the literature. Moreover, nano-switch is subjected to Casimir and electrostatic forces. Small scale and surface effects are also taken into account. Utilizing Hamilton's principle, governing equations are obtained and solved by Galerkin's method. A detailed parametric study is conducted to explain the small scale, surface layer, viscoelastic damping coefficient and applied voltage on the behavior of the pull-in voltage, time and deflection as well as pull-out voltage. The results is hoped to be useful in design and control of nano-electronic systems for engineering application even medical application in nano-surgical machinery.

## 2. Fundamental relations

### 2.1. Surface energy in nanoplate

According to the continuum surface elasticity theory [35] the surface strain energy in the plate can be expressed as:

$$U_s = \frac{1}{2}\int_{s^+} \tau_{\alpha\beta}\varepsilon_{\alpha\beta} ds^+ + \frac{1}{2}\int_{s^-} \tau_{\alpha\beta}\varepsilon_{\alpha\beta} ds^-, \tag{1}$$

in which $\tau_{\alpha\beta}$is the in-plane forces in different directions and operate on the nanoplate between bulk material and elastic surface which can be expressed as follows [36]:

$$\tau^s_{\alpha\beta} = \tau^s\delta_{\alpha\beta} + (\tau^s + \lambda^s)\varepsilon_{kk}\delta_{\alpha\beta} + 2(\mu^s - \tau^s)\varepsilon_{\alpha\beta} + \tau^s u^s_{\alpha,\beta}, \tag{2}$$

where $\tau^s$,$\delta_{\alpha\beta}$ and $u_\alpha$ are the residual stress under unconstrained conditions, Kronecker delta and the displacement field on the surface, respectively. Also, $\lambda^s = E^s\nu^s/(1-(\nu^s)^2)$ and $\mu^s = E^s/(2(1-\nu^s)$ are the Lame constants of surface layer where $E^s$ and $\nu^s$ are surface Yong's moduli and Poisson's ratio, respectively. It should be noted that the 's' superscript denotes the surface of the nanoplate.

The stress component $\sigma_{zz}$is neglected in contrast with the other components of stress in the applied theory. Nevertheless, this assumption does not satisfy the surface theory. Hence, it is supposed that $\sigma_{zz}$ satisfies the balance conditions on the upper and lower surfaces which may be calculated as [36]:

$$\sigma_{zz} = \frac{\left(\frac{\partial\tau^s_{xz}}{\partial x} + \frac{\partial\tau^s_{yz}}{\partial y} - \rho^s\frac{\partial^2 w}{\partial t^2}\right)|_{at\ top} + \left(\frac{\partial\tau^s_{xz}}{\partial x} + \frac{\partial\tau^s_{yz}}{\partial y} - \rho^s\frac{\partial^2 w}{\partial t^2}\right)|_{at\ bottom}}{2} + \frac{\left(\frac{\partial\tau^s_{xz}}{\partial x} + \frac{\partial\tau^s_{yz}}{\partial y} - \rho^s\frac{\partial^2 w}{\partial t^2}\right)|_{at\ top} - \left(\frac{\partial\tau^s_{xz}}{\partial x} + \frac{\partial\tau^s_{yz}}{\partial y} - \rho^s\frac{\partial^2 w}{\partial t^2}\right)|_{at\ bottom}}{2} z. \tag{3}$$

where $\rho^s$ is the density of the surface and

$$\tau^s_{\alpha z} = \tau^s u^s_{z,\alpha}, \quad \alpha,\beta = x,y \tag{4}$$

### 2.2. Nonlocal elasticity theory

The Eringen's nonlocal elasticity theory [26] considers the small scale effect in the continuum model. According to this theory, the stress at a reference point depends on all other points of the continuum model. The nonlocal equation of stress-strain relations are expressed as:

$$\left(1-(e_0a)^2\nabla^2\right)\sigma^{nl} = \sigma^l, \tag{5}$$

where $\sigma^l$ and $\sigma^{nl}$are the local and nonlocal stress tensor, respectively;$\nabla^{2-}$ is the Laplace operator in two dimensional Cartesian coordinates; $e_0a$ is the nonlocal parameter. Considering $\sigma_{zz}$from Eq. (3), the nonlocal stress-strain relations of the nanoplate are expressed as [37]:

$$\left(1-(e_0a)^2\nabla^2\right)\begin{bmatrix}\sigma_{xx}\\ \sigma_{yy}\\ \tau_{xz}\\ \tau_{yz}\\ \tau_{xy}\end{bmatrix} = \begin{bmatrix} C_{11}-\frac{(C_{13})^2}{C_{33}} & C_{12}-\frac{C_{13}C_{23}}{C_{33}} & 0 & 0 & 0\\ C_{12}-\frac{C_{13}C_{23}}{C_{33}} & C_{22}-\frac{(C_{23})^2}{C_{33}} & 0 & 0 & 0\\ 0 & 0 & C_{44} & 0 & 0\\ 0 & 0 & 0 & C_{55} & 0\\ 0 & 0 & 0 & 0 & C_{55}\end{bmatrix}\begin{bmatrix}\varepsilon_{xx}\\ \varepsilon_{yy}\\ \gamma_{xz}\\ \gamma_{yz}\\ \gamma_{xy}\end{bmatrix} + \begin{bmatrix}\frac{C_{13}}{C_{33}}\sigma_{zz}\\ \frac{C_{23}}{C_{33}}\sigma_{zz}\\ 0\\ 0\\ 0\end{bmatrix}, \tag{6}$$

in which $C_{ij}$ $i,j = 1,2,\ldots,6$ are elastic constants which are in term of Young's moduli, shear moduli and Poisson's ratio.

### 2.3. Strain energy based on sinusoidal shear deformation theory

The sinusoidal shear deformation theory considers transverse shear stress and free transverse shear stress conditions on the top and bottom surfaces of the plate without the shear correction factor. Based on this theory, the transverse displacement $w$ and the in-plane displacements

$u_x, v_y$ are given as [38]:

$$u_x(x,y,z,t) = -z\frac{\partial w_b}{\partial x} - \left(z - \frac{h}{\pi}\sin\frac{\pi z}{h}\right)\frac{\partial w_s}{\partial x}, \tag{7}$$

$$v_y(x,y,z,t) = -z\frac{\partial w_b}{\partial y} - \left(z - \frac{h}{\pi}\sin\frac{\pi z}{h}\right)\frac{\partial w_s}{\partial y}, \tag{8}$$

$$w(x,y,z,t) = w_b(x,y,t) + w_s(x,y,t), \tag{9}$$

where $w_b$ and $w_s$are bending and shear components of transverse displacement, respectively; $h$ is the thickness of the nanoplate. However, the strain-displacement relations can be obtained as follows:

$$\varepsilon_{xx} = -z\frac{\partial^2 w_b}{\partial x^2} - \left(z - \frac{h}{\pi}\sin\frac{\pi z}{h}\right)\frac{\partial^2 w_s}{\partial x^2}, \tag{10a}$$

$$\varepsilon_{yy} = -z\frac{\partial^2 w_b}{\partial y^2} - \left(z - \frac{h}{\pi}\sin\frac{\pi z}{h}\right)\frac{\partial^2 w_s}{\partial y^2}, \tag{10b}$$

$$\gamma_{xy} = -2z\frac{\partial^2 w_b}{\partial x\partial y} + 2\left(z - \frac{h}{\pi}\sin\frac{\pi z}{h}\right)\frac{\partial^2 w_s}{\partial x\partial y}, \tag{10c}$$

$$\gamma_{yz} = \cos\frac{\pi z}{h}\frac{\partial w_s}{\partial y}, \tag{10d}$$

$$\gamma_{xz} = \cos\frac{\pi z}{h}\frac{\partial w_s}{\partial x}. \tag{10f}$$

The bulk strain energy of the nanoplate based on the sinusoidal shear deformation theory can be written as:

$$U_b = \int_V \left(\sigma_x\varepsilon_{xx} + \sigma_y\varepsilon_{yy} + \sigma_{xy}\gamma_{xy} + \sigma_{xz}\gamma_{xz} + \sigma_{yz}\gamma_{yz}\right)dAdz =$$
$$U_b = \int_A \begin{pmatrix} -M^b_{xx}\frac{\partial^2 w_b}{\partial x^2} - M^s_{xx}\frac{\partial^2 w_s}{\partial x^2} - M^b_{yy}\frac{\partial^2 w_b}{\partial y^2} - M^s_{yy}\frac{\partial^2 w_s}{\partial y^2} - 2M^b_{xy}\frac{\partial^2 w_b}{\partial x\partial y} - 2M^s_{xy}\frac{\partial^2 w_s}{\partial x\partial y} \\ +Q_{yz}\frac{\partial w_s}{\partial y} + Q_{xz}\frac{\partial w_s}{\partial x} \end{pmatrix} dA, \tag{11}$$

where the stress resultants in the middle surface of nanoplate can be defined as:

$$\begin{aligned} \left(M^b_i, M^s_i\right) &= \int_{-\frac{h}{2}}^{\frac{h}{2}} (z,f)\sigma_i dz, \quad i = xx, yy, xy, \\ Q_i &= \int_{-\frac{h}{2}}^{\frac{h}{2}} \left(\cos\frac{\pi z}{h}\right)\sigma_i dz, \quad i = xz, yz. \end{aligned} \tag{12}$$

where $f = -z + \frac{h}{\pi}\sin\frac{\pi z}{h}$. Therefore, the strain energy of the nanoplate including the surface and the bulk potential energies can be written as

$$U = U_b + U_s, \tag{13}$$

where $U_b$and $U_s$are bulk and surface potential energies, respectively.

### 2.4. Viscoelastic model

Based on Kelvin-Voigt's model on elastic materials, assuming the Poisson's ratio to be constant, the elastic constants should be replaced with $C_{ij}(1 + g\frac{\partial}{\partial t})$ where $g$ is the viscoelastic structural damping coefficient [39].

### 2.5. External works

#### 2.5.1. Electrostatic force

Fig. 1(a) shows the schematic diagram of nano-switch consists of two components that one of them is fixed and the other is movable. They are separated by a dielectric spacer with an initial gap $g_0$. $a$,$b$ and$h$ are the length, width and thickness of the nanoplate, respectively. Two type of boundary conditions namely as CCCC and CCFF are considered which are shown in Fig. 1(b).

By applying voltage $v$, two forces of electrostatic force $F_e$ and intermolecular Casimir force$F_c$ are produced that makes the nanoplate deflects toward the fixed electrode. The electrostatic force per unit length can be written as [28]:

$$F_e = \frac{\varepsilon_0 b v^2}{2(g_0 - w)^2}\left(1 + 0.65\frac{g_0 - w}{b}\right), \tag{14}$$

in which $\varepsilon_0 = 8.854\times10^{-12} F/m$ is the permittivity of vacuum; $v$is the DC voltage that applied between the nanoplate and stationary electrode; $g_0$ is the initial gap between the nanoplate and infinite ground plane.

#### 2.5.2. Casimir force

The dielectric spacer is assumed to be larger than 20 nm to calculate the inter molecular forces between two components by the Casimir force as [28]:

$$F_c = \frac{\pi^2\hbar c b}{240(g_0 - w)^4}, \tag{15}$$

where $c = 3\times10^8 m/s$ is the speed of light, $\hbar = 1.055\times10^{-34} J\cdot s$ is the Planck's constant divided by 2π. Consequently, the external work due to the intermolecular and electrostatic can be are written as:

$$V = \frac{1}{2}\int_A (F_e + F_c)dA. \tag{16}$$

### 2.6. Kinetic energy

The total kinetic energy surface and bulk of the nanoplate is:

$$K = \frac{1}{2}\int_V \left(\dot{u_x}^2 + \dot{v_y}^2 + \dot{w}^2\right)\rho dV, \tag{17}$$

in this equation dot superscript denotes the differentiation with respect to the time variable and $\rho$ is the mass density of the nanoplate.

## 3. Solution method

### 3.1. Galerkin's method

In this study, Galerkin's method is utilized to solve the system of motion equations. The first mode of dynamic deflection of the nano-switch is assumed as [40]:

$$\begin{aligned} &[w_b(x,y,t), w_s(x,y,t)] = w_0(x,y)[u_b(t), u_s(t)], \\ &w_0(x,y) = \varphi(x)\psi(y), \end{aligned} \tag{18}$$

where $\varphi(x)$ and $\psi(y)$ are normalized eigen functions in which satisfied all of the boundary conditions;$u(t)$ is an unknown time-dependent deflection parameter of the nanoplate. For example $\varphi(x)$ and $\psi(y)$ can be assumed as [41]:

$$\begin{aligned}\varphi(x) &= (\cos(\beta x) - \cosh(\beta x)) - \frac{\cos(\beta a) + \cosh(\beta a)}{\sin(\beta a) + \sinh(\beta a)}(\sin(\beta x) - \sinh(\beta x)),\ \beta = 1.8751,\\ \psi(y) &= (\cos(\mu y) - \cosh(\mu y)) - \frac{\cos(\mu a) - \cosh(\mu a)}{\sin(\mu a) - \sinh(\mu a)}(\sin(\mu y) - \sinh(\mu y)),\ \mu = 4.7300.\end{aligned} \tag{19}$$

Eq. (19) is the first eigen function of a CCFF nanoplate.

### 3.2. Motion equations

Based on Hamilton's principle, the variational form of motion equations can be expressed by [21]:

$$\int_{0_1}^{T} [\delta U + \delta V - \delta K]\, dt = 0. \tag{20}$$

Substituting Eqs. (13), (16) and (17) into Eq. (20), motion equations are obtained. Following parameters are defined to change the motion equations in a dimensionless form:

$$\begin{aligned}&k_1 = \frac{\varepsilon_0 v^2}{2E_1 g_0^2}, \quad \bar{\mu}_s = \frac{\mu^s}{E_1 h}, \quad \bar{\tau}_s = \frac{\tau^s}{E_1 h}, \quad \bar{\lambda}_s = \frac{\lambda^s}{E_1 h},\\ &g_v = \frac{g}{a^2}\sqrt{\frac{E_1 h^2}{\rho}}, \quad k_2 = \frac{\pi^2 ch}{240 E_1 g_0^4}, \quad \bar{\rho}_s = \frac{\rho^s}{\rho a}, \quad \bar{g}_0 = \frac{g_0}{h},\\ &\beta = \frac{E_2}{E_1}, \quad \tau = \frac{t}{a}\sqrt{\frac{E_1}{\rho}}, \quad \Gamma = \frac{h}{a}, \quad Y = \frac{y}{a},\\ &X = \frac{x}{a}, \quad \gamma = \frac{a}{b}, \quad W_b = \frac{w_b}{h}, \quad W_s = \frac{w_s}{h}, \quad \mu = \frac{(e_0 a)^2}{a^2}, \quad V = va^2\sqrt{\frac{\varepsilon_0}{g_0^3 E h^3}}.\end{aligned} \tag{21}$$

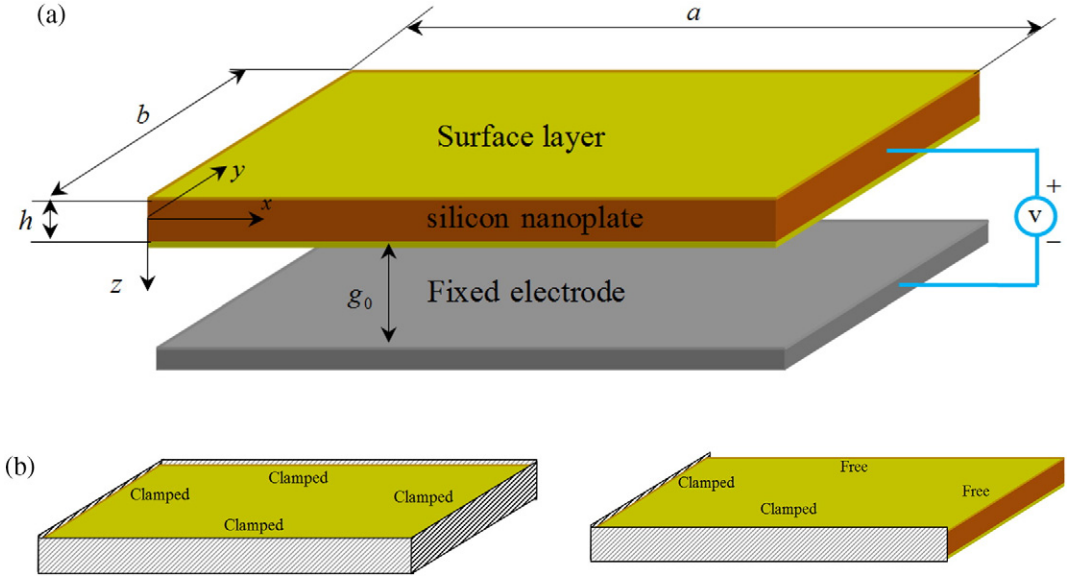



**Fig. 1.** (a) Schematic of an electrostatically actuated nanoplate with surface layers, (b) boundary conditions.

Therefore, the non-dimensional form of motion equations by collecting the coefficients of $\delta w_b$ and $\delta w_s$ can be written as:

$$\begin{aligned}
&\delta w_i: \\
&\left\{\overline{D}_{xbi}\frac{\partial^4 W_b}{\partial X^4}+\overline{D}_{xsi}\frac{\partial^4 W_s}{\partial X^4}+\overline{D}_{xybi}\frac{\partial^4 W_b}{\partial X^2\partial Y^2}+\overline{D}_{xysi}\frac{\partial^4 W_s}{\partial X^2\partial Y^2}+\overline{D}_{ybi}\frac{\partial^4 W_b}{\partial Y^4}+\overline{D}_{ysi}\frac{\partial^4 W_s}{\partial Y^4}\right\}u(\tau)+\\
&\left\{\begin{array}{l}\overline{D}_{xbgi}g_v\frac{\partial^4 W_b}{\partial X^4}+\overline{D}_{xsgi}g_v\frac{\partial^4 W_s}{\partial X^4}+\overline{D}_{xybgi}g_v\frac{\partial^4 W_b}{\partial X^2\partial Y^2}+\\ \overline{D}_{xysgi}g_v\frac{\partial^4 W_s}{\partial X^2\partial Y^2}+\overline{D}_{ybgi}g_v\frac{\partial^4 W_b}{\partial Y^4}+\overline{D}_{ysgi}g_v\frac{\partial^4 W_s}{\partial Y^4}\end{array}\right\}\dot{u}(\tau)+\\
&\left\{\begin{array}{l}\bar{I}_0+\bar{I}_{xbi}\frac{\partial^2 W_b}{\partial X^2}+\bar{I}_{xsi}\frac{\partial^2 W_s}{\partial X^2}+\bar{I}_{ybi}\frac{\partial^2 W_b}{\partial Y^2}+\bar{I}_{ysi}\frac{\partial^2 W_s}{\partial Y^2}\\ \bar{I}_{2bi}\frac{\partial^4 W_b}{\partial X^4}+\bar{I}_{2si}\frac{\partial^4 W_s}{\partial X^4}+\bar{I}_{3bi}\frac{\partial^4 W_b}{\partial X^2\partial Y^2}+\bar{I}_{3si}\frac{\partial^4 W_s}{\partial X^2\partial Y^2}+\\ \bar{I}_{4bi}\frac{\partial^4 W_b}{\partial Y^4}+\bar{I}_{4si}\frac{\partial^4 W_s}{\partial Y^4}\end{array}\right\}\ddot{u}(\tau)=Q_i,\\
&i=b,s
\end{aligned} \tag{22}$$

where $Q_i$ is expressed as:

$$\begin{aligned}
&Q_i=k_2+(1+0.65g_0)k_1+(4k_2+(2+0.65g_0)k_1)\frac{u(\tau)}{\bar{g}_0}(W_b+W_s)\\
&(10k_2+(3+0.65g_0)k_1)\frac{u^2(\tau)}{{\bar{g}_0}^2}(W_b+W_s)^2-\\
&\lambda^2\left[\begin{array}{l}(4k_2+(2+0.65g_0)k_1)\frac{u(\tau)}{\bar{g}_0}\left(\left(\frac{\partial^2 W_b}{\partial X^2}+\frac{\partial^2 W_b}{\partial Y^2}\right)+\left(\frac{\partial^2 W_s}{\partial X^2}+\frac{\partial^2 W_s}{\partial Y^2}\right)\right)\\ (10k_2+(3+0.65\bar{g}_0)k_1)\frac{u^2(\tau)}{{\bar{g}_0}^2}\left(\begin{array}{l}\left(2\left(\frac{\partial W_b}{\partial X}\right)^2+2W_b\frac{\partial^2 W_b}{\partial X^2}+2\left(\frac{\partial W_b}{\partial Y}\right)^2+2W_b\frac{\partial^2 W_b}{\partial Y^2}\right)+\\ \left(2\left(\frac{\partial W_s}{\partial X}\right)^2+2W_s\frac{\partial^2 W_s}{\partial X^2}+2\left(\frac{\partial W_s}{\partial Y}\right)^2+2W_s\frac{\partial^2 W_s}{\partial Y^2}\right)+\\ 2\left(W_b\left(\frac{\partial^2 W_s}{\partial X^2}+\frac{\partial^2 W_s}{\partial Y^2}\right)+W_s\left(\frac{\partial^2 W_b}{\partial X^2}+\frac{\partial^2 W_b}{\partial Y^2}\right)\right)\end{array}\right)\end{array}\right].
\end{aligned} \tag{23}$$

It is worth to mention that for the sake of brevity, the special parameters such as $\overline{D}_{xbi}$, $\overline{D}_{xbgi}$, $\overline{D}_{xybi}$, $\overline{D}_{xybgi}$ and dimensionless moment of inertia are given in Appendix A.

Substituting Eq. (23) into Eq. (22), multiplying the weight functions $W(X,Y)$, and double integrating it over the interval of 0 and 1, the Galerkin's procedure leads to the following two nonlinear time dependent second-order ordinary differential equation for $W_s$ and $W_b$ as follows:

$$\begin{bmatrix}K_{bb} & K_{bs}\\ K_{sb} & K_{ss}\end{bmatrix}\begin{bmatrix}u_b\\ u_s\end{bmatrix}+\begin{bmatrix}C_{bb} & C_{bs}\\ C_{sb} & C_{ss}\end{bmatrix}\begin{Bmatrix}\dot{u}_b\\ \dot{u}_s\end{Bmatrix}+\begin{bmatrix}M_{bb} & M_{bs}\\ M_{sb} & M_{ss}\end{bmatrix}\begin{Bmatrix}\ddot{u}_b\\ \ddot{u}_s\end{Bmatrix}=\begin{Bmatrix}f_b\\ f_s\end{Bmatrix}+\begin{bmatrix}K_{2,bb} & K_{2,bs}\\ K_{2,sb} & K_{2,ss}\end{bmatrix}\begin{Bmatrix}u_b^2\\ u_s^2\end{Bmatrix}+\begin{bmatrix}K_{3,bb} & K_{3,bs}\\ K_{3,sb} & K_{3,ss}\end{bmatrix}\begin{Bmatrix}u_b^3\\ u_s^3\end{Bmatrix}, \tag{24}$$

where $f_i$ can be written as:

$$\begin{aligned}
&f_i=\int_0^1\int_0^1 F_i\times W(X,Y)dXdY,\\
&i=(b,s),
\end{aligned} \tag{25}$$

where $K$, $M$ and $C$ are stiffness, mass and damping coefficients, respectively, which are defined as:

$$\begin{aligned}
K_{bi}&=\int_0^1\int_0^1\left((D_{xbi}+D_{xsi})\frac{\partial^4 W_i(X,Y)}{\partial X^4}+(D_{ybi}+D_{ysi})\frac{\partial^4 W_i(X,Y)}{\partial Y^4}+(D_{xybi}+D_{xysi})\frac{\partial^4 W_i(X,Y)}{\partial X^2\partial Y^2}\right)W(X,Y)dYdX,\\
K_{si}&=\int_0^1\int_0^1\left((D_{xbi}+D_{xsi})\frac{\partial^4 W_i(X,Y)}{\partial X^4}+(D_{ybi}+D_{ysi})\frac{\partial^4 W_i(X,Y)}{\partial Y^4}+(D_{xybi}+D_{xysi})\frac{\partial^4 W_i(X,Y)}{\partial X^2\partial Y^2}\right)W(X,Y)dYdX,
\end{aligned} \tag{26}$$

$$\begin{aligned}
K_{2,mn}&=\int_0^1\int_0^1\left(1-(e_0a)^2\nabla^2\right)W(X,Y)^2W(X,Y)dYdX,\\
K_{3,mn}&=\int_0^1\int_0^1\left(1-(\lambda)^2\nabla^2\right)W(X,Y)^3W(X,Y)dYdY,\\
&mn=(b,s),
\end{aligned} \tag{27}$$

$$M_{bi} = \int_0^1 \int_0^1 \left( \bar{I}_0 W(X,Y) + (\bar{I}_{xbi} + \bar{I}_{xsi}) \frac{\partial^2 W(X,Y)}{\partial X^2} + (\bar{I}_{ybi} + \bar{I}_{ysi}) \frac{\partial^2 W(X,Y)}{\partial Y^2} + (\bar{I}_{2bi} + \bar{I}_{2si}) \frac{\partial^4 W(X,Y)}{\partial X^4} + (\bar{I}_{3bi} + \bar{I}_{3si}) \frac{\partial^4 W(X,Y)}{\partial X^2 \partial Y^2} + (\bar{I}_{4bi} + \bar{I}_{4si}) \frac{\partial^4 W(X,Y)}{\partial Y^4} \right) W(X,Y) dY dX,$$

$$M_{si} = \int_0^1 \int_0^1 \left( \bar{I}_0 W(X,Y) + (\bar{I}_{xbi} + \bar{I}_{xsi}) \frac{\partial^2 W(X,Y)}{\partial X^2} + (\bar{I}_{ybi} + \bar{I}_{ysi}) \frac{\partial^2 W(X,Y)}{\partial Y^2} + (\bar{I}_{2bi} + \bar{I}_{2si}) \frac{\partial^4 W(X,Y)}{\partial X^4} + (\bar{I}_{3bi} + \bar{I}_{3si}) \frac{\partial^4 W(X,Y)}{\partial X^2 \partial Y^2} + (\bar{I}_{4bi} + \bar{I}_{4si}) \frac{\partial^4 W(X,Y)}{\partial Y^4} \right) W(X,Y) dY dX, \quad (i = (b,s)) \tag{28}$$

$$C_{bi} = \int_0^1 \int_0^1 \left( (D_{xbgi} + D_{xsgi}) \frac{\partial^4 W(X,Y)}{\partial X^4} + (D_{ybgi} + D_{ysgi}) \frac{\partial^4 W(X,Y)}{\partial Y^4} + (D_{xybgi} + D_{xysgi}) \frac{\partial^4 W(X,Y)}{\partial X^2 \partial Y^2} \right) \bar{g} W(X,Y) dY dX,$$

$$C_{si} = \int_0^1 \int_0^1 \left( (D_{xbgi} + D_{xsgi}) \frac{\partial^4 W(X,Y)}{\partial X^4} + (D_{ybgi} + D_{ysgi}) \frac{\partial^4 W(X,Y)}{\partial Y^4} + (D_{xybgi} + D_{xysgi}) \frac{\partial^4 W(X,Y)}{\partial X^2 \partial Y^2} \right) \bar{g} W(X,Y) dY dX. \tag{29}$$

Considering definite initial condition, Eq. (24) is solved by Matlab software numerically. It should be noted that boundary conditions on each edge of movable electrode are the combination of clamped (C) and free (F) edges. In the following section, the effect of various parameters on CCCC and CCFF nanoplate are discussed in detail.

## 4. Results and discussion

In this work, the viscoelastic nanoplate is considered as a nano-switch and the dynamic pull-in and pull-out analysis of it, is studied under electrostatic and intermolecular Casimir forces. Using sinusoidal shear deformation theory, various parameters such as nonlocal parameter, surface layer, viscoelastic damping and applied voltage on the pull-in voltage, time and deflection as well as pull-out voltage of nanoplate are discussed. For this purpose, a silicon nanoplate with length to thickness ratio of $a/h = 10$ and length to width ratio of $a/b = 2$ is selected by the elastic and surface material properties listed in Table 1.

### 4.1. Validation

As regards validation of our obtained results, Table 2 compares the present results neglecting transverse shear deformation and surface effects with numerical and experimental results of Mousavi et al. [42] using DQM. This comparison is done in Pull-in parameter of $\beta = \frac{\varepsilon_0 b V^2 a^4}{2g^3 EI}$ applying the intermolecular forces and considering the small scale effects. It can be observed that the present results have the excellent agreement with the numerical results reported by Mousavi et al. [42], indicating validation of this work.

### 4.2. Pull-in voltage

Fig. 2(a) and (b) present the effect of dimensionless viscoelastic damping coefficient ($g_v$) and dimensionless nonlocal parameter ($\mu$) on

**Table 1**
Elastic properties of the silicon nanoplate [36].

| Bulk material properties | Surface material properties |
|---|---|
| $E = 210\ GPa$ | $E^s = -10.036$ N/m |
| $\nu = 0.24$ | $\nu^s = 0$ |
| $\rho = 2331\ Kg/m^3$ | $\rho^s = 3.17 \times 10^{-7}\ Kg/m^2$ |
| | $\tau^s = 5.60\ N/m$ |

**Table 2**
Compression of dimensionless pull-in parameter $\beta = \frac{\varepsilon_0 b V^2 L^4}{2g^3 EI}$ with different nonlocal parameters.

| Method | $\mu = 0$ | $\mu = 0.1$ | $\mu = 0.2$ | $\mu = 0.3$ |
|---|---|---|---|---|
| Present work (Galerkin) | 49.17 | 46.21 | 38.75 | 31.15 |
| Mousavi et al. (DQM) [42] | 51.81 | 49.84 | 41.47 | 32.81 |

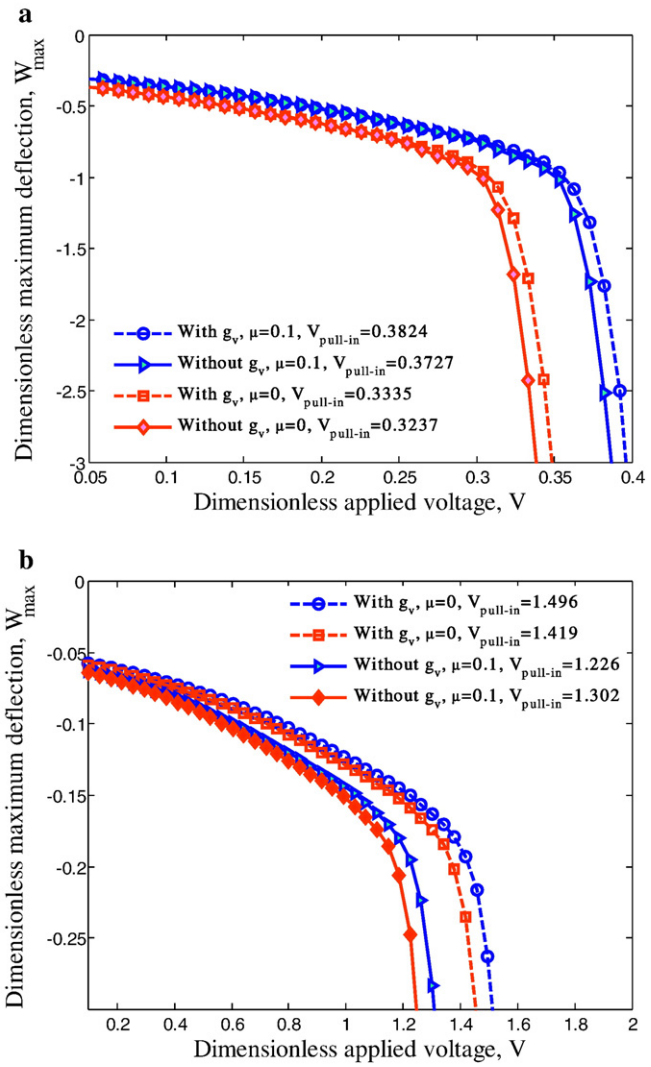



**Fig. 2.** a. Effects of structural damping and nonlocal parameters on the pull-in voltage for CCFF nanoplate. b. Effects of structural damping and nonlocal parameters on the pull-in voltage for CCCC nanoplate.

the graph of dimensionless maximum deflection versus the dimensionless applied voltage ($V$) for CCFF and CCCC nanoplates, respectively. When the applied voltage increases beyond a critical value, called pull-in voltage, the elastic force can no longer resist the electrostatic force, thereby leading to collapse of the nanoplate. In this state, the displacement increases sharply and hence the pull-in displacement will be occurred. As can be seen, considering the structural damping effects leads to higher deflection and pull-in voltage for the both cases of CCFF and CCCC nanoplates.

It can be seen from Fig. 2(a) that the nonlocal parameter increases the pull-in voltage and decreases the pull-in deflection. However, it can be concluded that considering small scale effects makes the structure stiffer and delays its pull-in instability. This phenomenon is converse for the CCCC nanoplate as shown in Fig. 2(b) where with considering the nonlocal parameter, the pull-in voltage decreases and the pull-in deflection increase. So, in the CCCC nanoplate, increasing the nonlocal parameter leads to softer structure. Comparing the pull-in voltage and deflection of the CCFF and CCCC nanoplates, it can be found that because of such strong fixed end boundary condition of CCCC nanoplate, the structure collapse in the higher voltages than the CCFF nanoplate.

Fig. 3(a) and (b) illustrate the effects of Casmir force and nonlocal parameter on the dimensionless pull-in voltage and deflection for the CCCFF and CCCC nanoplates, respectively. As shown in both figures, Casimir force plays an important role in the instability of the structure. It is observed that the pull-in deflection and pull-in voltage of the nano-switche are increased and decreased, respectively considering the Casimir force. It is due to the fact that the Casimir force is related to the inverse fourth power of the separation gap which leads to act higher force on the nanoplate. Hence, the structure subjected to Casimir force collapses at lower voltages. With respect to the effect of the nonlocal parameter on the pull-in instability of the structure, it can be seen that considering size-effects leads to higher and lower pull-in voltage for the CCFF and CCCC nanoplates, respectively. Noted that mentioned phenomenon is converse for the pull-in deflection of the nano-switche.

Surface stress effects of the nanoplate are shown in Fig. 4(a) and (b) on the dimensionless pull-in voltage and deflection of the nano-switche for the CCFF and CCCC nanoplates, respectively. The difference between curves with surface effect and without it demonstrates that by considering the surface stress effects, the structure collapses at higher voltages. In other words, considering surface stress effects leads to higher bending stiffness and consequently decreases in the deflection of the structure. Overall, it is evident that instability of nanoplate with CCCC boundary condition is occurred at higher voltages with respect to the nanoplate with CCFF boundary condition.

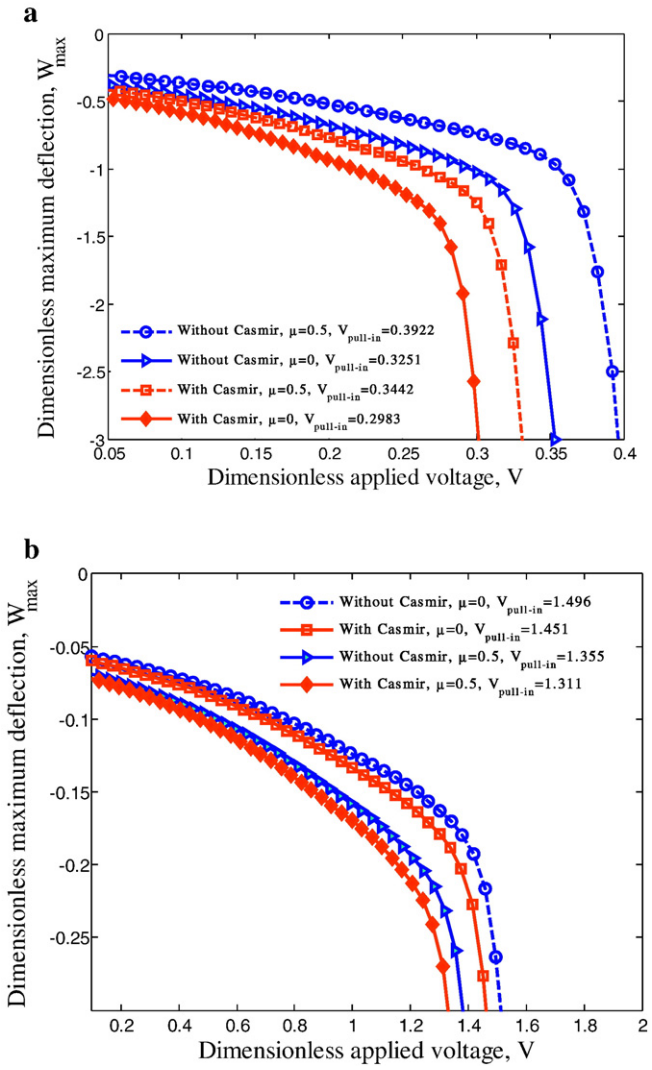



**Fig. 3.** a. Effects of Casimir force and nonlocal parameter on the pull-in voltage for CCFF nanoplate. b. Effects of Casimir force and nonlocal parameter on the pull-in voltage for CCCC nanoplate.

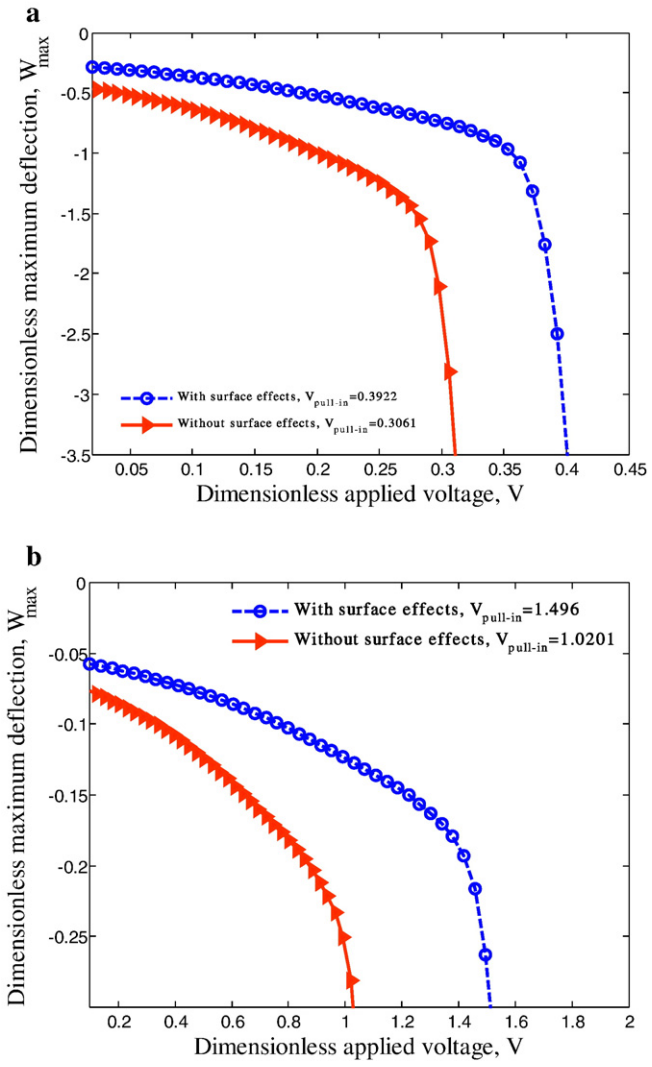



**Fig. 4.** a. Effects of surface stress on the pull-in voltage for CCFF nanoplate. b. Effects of surface stress on the pull-in voltage for CCCC nanoplate.

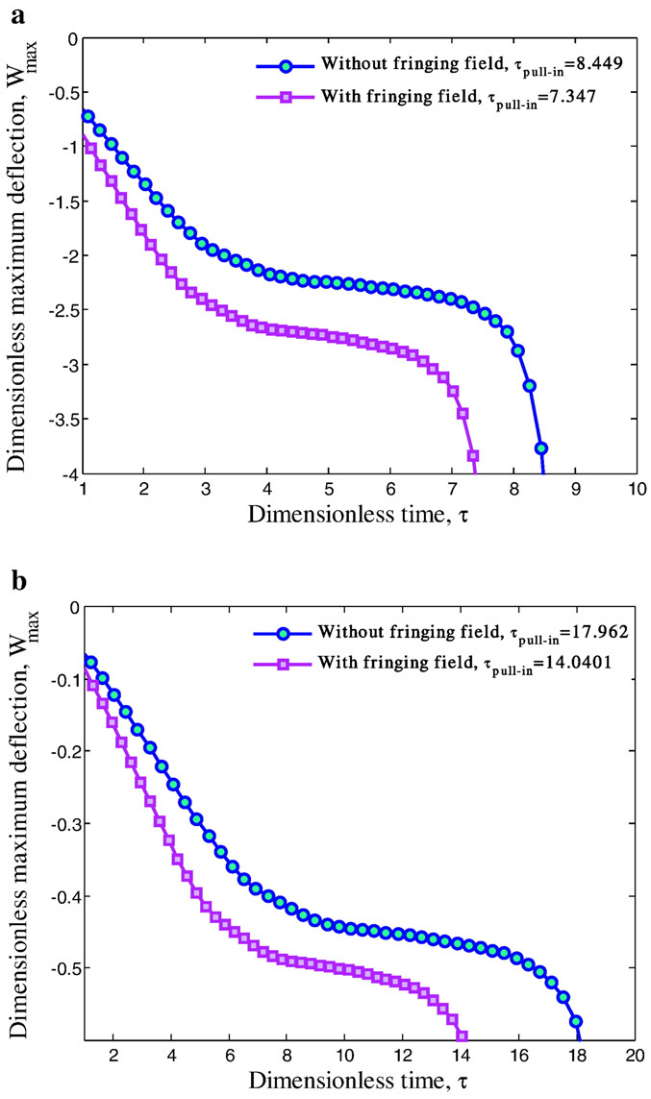



**Fig. 5.** a. Effects of fringing fields on the pull-in time for CCFF nanoplate. b. Effects of fringing fields on the pull-in time for CCCC nanoplate.

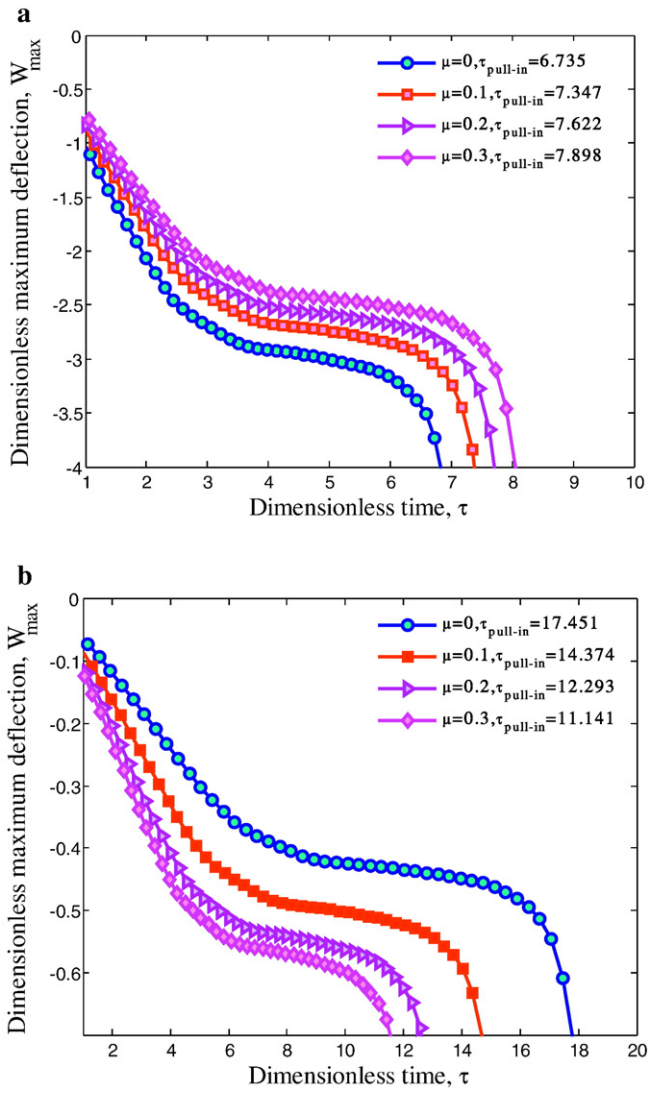



**Fig. 6.** a. Effects of nonlocal parameter on the pull-in time for CCFF nanoplate. b. Effects of nonlocal parameter on the pull-in time for CCCC nanoplate.

### *4.3. Pull-in time*

When the pull-in phenomenon occurs, the pull-in delay time is another parameter we should concern about. Fig. 5(a) and (b) present the effect of fringing field on the history curves of the maximum transverse displacement for the CCFF and CCCC nanoplates, respectively. It should be noted that the second term of Eq. (14), $(0.65)\frac{\varepsilon_0 v^2}{2(g_0-w)}$, is fringing field force and as can be seen from these figures has great effect on the pull-in phenomenon of the nano-switche. As shown in Fig. 5(a) and (b), fringing field effect decreases the pull-in delay time and slightly increases the pull-in deflection. Furthermore, due to the more stiffness of the nanoplate with CCCC boundary condition, the pull-in delay time of the nano-switche is later than the nanoplate with CCFF boundary condition.

Fig. 6(a) and (b) demonstrate the effect of dimensionless nonlocal parameter on the pull-in delay time of the nano-switche, respectively for the CCFF and CCCC boundary conditions. These figures indicate that the nonlocal parameter has a dramatic effect on the pull-in instability of the structure. It is obvious that increasing nonlocal parameters will shorten the pull-in delay time for the CCCC nanoplate. For the CCFF nanoplate, the pull-in delay time is increases with increasing nonlocal parameters. In addition, the nano-switche with CCCC boundary condition will collapse later with respect to the nano-switche with CCFF one. This is physically reasonable since the structure with CCCC boundary condition has higher stiffness.

The higher order shear effect on the pull-in delay time of the CCFF and CCCC nano-switche is shown in Fig. 7(a) and (b), respectively. It can be seen that considering shear effects has an important effect on the pull-in behavior of the structure. However, considering shear effects leads to a system with more degree of freedom and consequently, the deflection of the nano-switche increases and the pull-in delay time decreases. The aforementioned phenomenon is the same for both boundary conditions of CCFF and CCCC.

### *4.4. Pull-out voltage*

Pull-out problem begins after the structure collapses to the substrate. In this state, a new force namely as stiction force is existed which is due to the Casimir force in this work. So reducing applied voltage, nanoplate pull-out from dielectric when the elastic restoring force of nanoplate balances with the total of electrostatic and stiction forces. Fig. 8(a) and (b) present the effects of nonlocal parameter and surface stress on the curves of dimensionless pull-out voltage as a function of

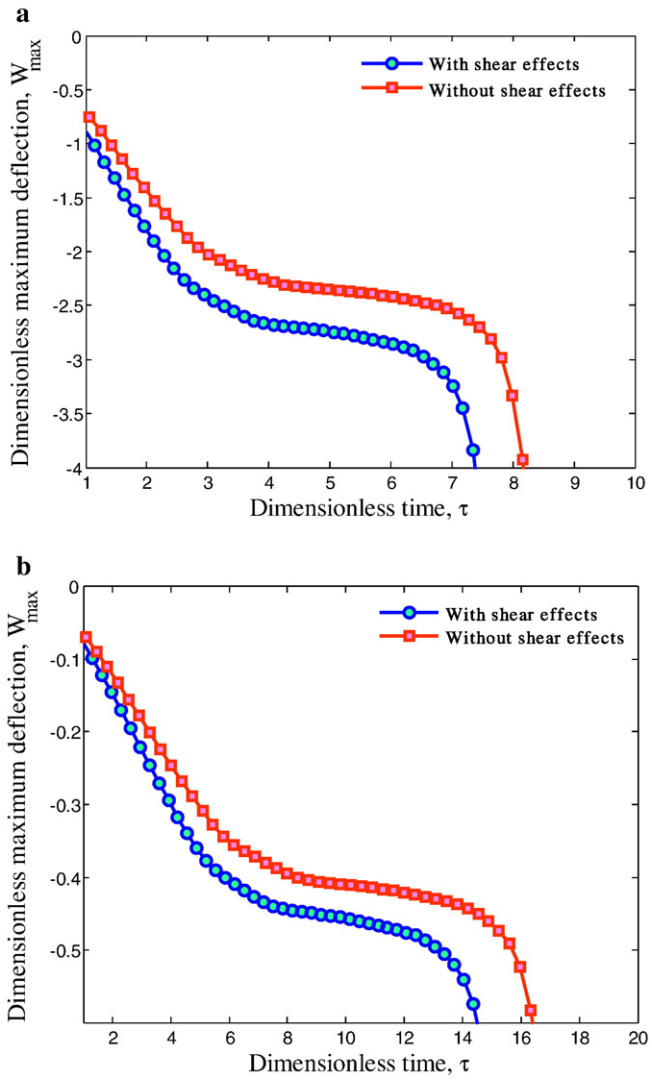



**Fig. 7.** a. Effects of higher order shear on the pull-in time for CCFF nanoplate. b. Effects of higher order shear on the pull-in time for CCCC nanoplate.

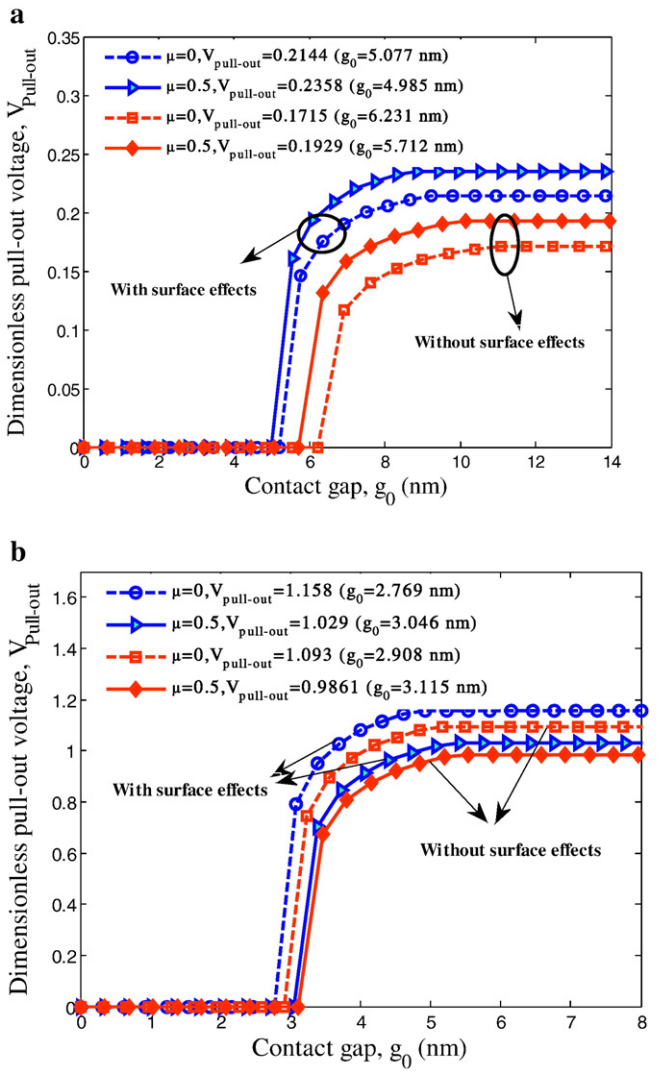



**Fig. 8.** a. Effects of nonlocal parameter and surface stress on the pull-out voltage for CCFF nanoplate. b. Effects of nonlocal parameter and surface stress on the pull-out voltage for CCCC nanoplate.

contact gap ($g_0$) for the CCFF and CCCC nanoplates, respectively. It can be found that the pull-out voltage sharply falls to zero at a special contact gap which is very important in design of nano-switche. For example, in the case of considering surface effect and $\mu = 0.5$ for the CCFF and CCCC nanoplates, the contact gaps related to the pull-out voltage are 4.985 nm and 3.046 nm, respectively. This physically means that, for the present nano-switche, if the contact gap becomes less than 4.985 nm and 3.046 nm, respectively for the CCFF and CCCC nanoplates, there is considerable probability that the nanoplate may not release at all. However, it is assumed the contact gap equal to 7 nm for the CCFF nano-switche and 4 nm for the CCCC ones. In addition, considering surface effects makes the structure stiffer and consequently, the pull-out voltage of the nano-switche increases and the related contact gap is decreased. It is also observed that increasing the nonlocal parameter, the pull-out voltage and the corresponding contact gap are increased and decreased, respectively for the CCFF nanoplate while the mentioned phenomenon is converse for the CCCC nanoplate.

In order to show the effect of the stiction force on the pull-out voltage of the structure, Fig. 9(a) and (b) are plotted, respectively for the CCFF and CCCC nano-switche. It is obtained that the pull-out voltage of the CCFF and CCCC nanoplates is 0.2701 V and 2.286 V, respectively without considering stiction force. These values are obtained from consideration of the electrostatic force only and thus determine the upper boundary of the pull-out voltage. However, considering the stiction force leads to decrease in the pull-out voltage of the nano-switch. Noted that this result is the same as that reported by Chakraborty et al. [34], indicating validation of this study.

## 5. Conclusion

In this study, dynamic pull-in and pull-out behaviors of a viscoelastic nano-switch was carried out based on sinusoidal shear deformation theory. Nano-switch was made of silicon and subjected to Casimir and electrostatic forces. Using Eringen's nonlocal elasticity theory, the effect of small scale was taken into account. Based on energy method, motion equations were obtained and solved using Galerkin's method considering surface stress effects based on Gurtin-Murdoch theory. The influences of different parameters such as nonlocal parameter, surface layer, structural damping and applied voltage on the pull-in voltage, pull-in time, pull-in deflection and pull-out voltage were studied. The results can be used in design of nano-electromechanical systems such

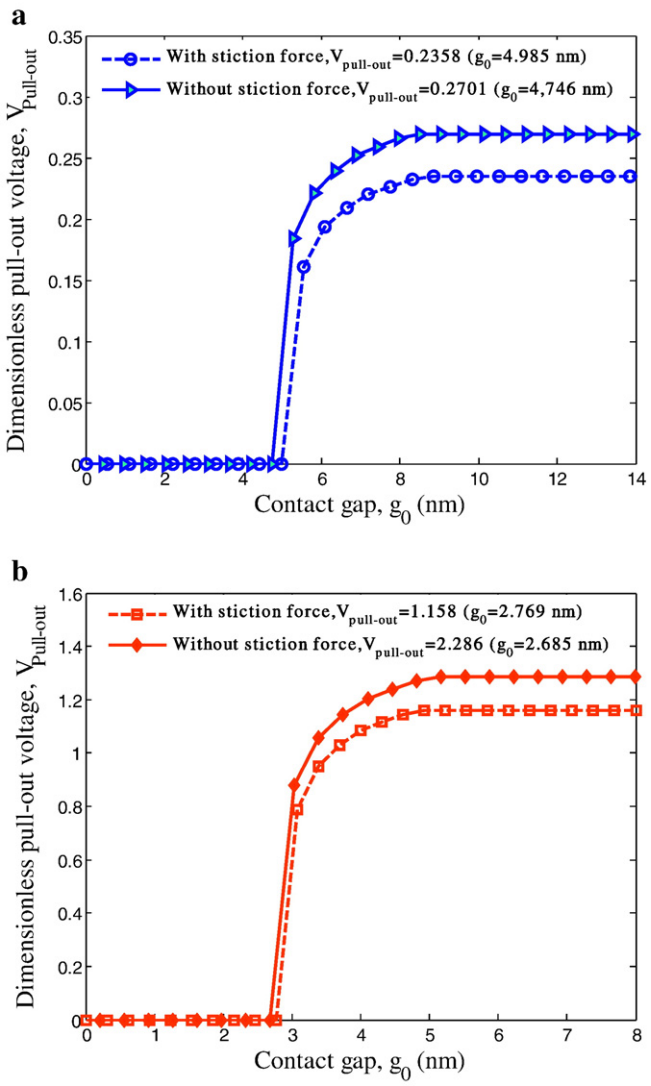



**Fig. 9.** a. Effects of stiction force on the pull-out voltage for CCFF nanoplate. b. Effects of stiction force on the pull-out voltage for CCCC nanoplate.

as nano-switch, nano-sensors and nano-actuators. The most important conclusions of this work are:

1. In the presence of Casimir force as absorbing tensile forces, the instability happens in the lower pull-in voltages.
2. The pull-in voltage and time as well as pull-out voltage of nano-switch with CCCC boundary condition were occurred in higher voltage and time than CCFF boundary condition.
3. Considering the structural damping effects leads to higher deflection and pull-in voltage for the both cases of CCFF and CCCC nanoplates.
4. With considering the size effects, the pull-in voltage, pull-in time and pull-out voltage decrease for CCCC nanoplate and increase for CCFF ones.
5. Considering the surface stress effects, the structure collapses and pull-out at higher voltages.
6. Fringing field effect decreases the pull-in delay time and slightly increases the pull-in deflection.
7. In the case of considering surface effect and $\mu = 0.5$ for the CCFF and CCCC nanoplates, the contact gaps related to the pull-out voltage are 4.985 nm and 3.046 nm, respectively.
8. Considering the stiction force leads to decrease in the pull-out voltage of the nano-switch.

## Appendix A

$$\overline{D}_{xbs} = \left(\left(\frac{1}{12}-\frac{2}{\pi^3}\right)\left(\frac{\Gamma^4}{1-\nu_{21}\nu_{12}}\right)+(2\mu^s+\lambda^s)\Gamma^4\right),$$
$$\overline{D}_{xss} = \left(\left(\frac{1}{12}-\frac{4}{\pi^3}+\frac{1}{2\pi^2}\right)\left(\frac{\Gamma^4}{1-\nu_{21}\nu_{12}}\right)+(2\mu^s+\lambda^s)\Gamma^4\right), \quad (A1)$$

$$\overline{D}_{xbgs} = \left(\frac{1}{12}-\frac{2}{\pi^3}\right)\left(\frac{\Gamma^3}{1-\nu_{21}\nu_{12}}\right),$$
$$\overline{D}_{xsgs} = \left(\frac{1}{12}-\frac{4}{\pi^3}+\frac{1}{2\pi^2}\right)\left(\frac{\Gamma^3}{1-\nu_{21}\nu_{12}}\right), \quad (A2)$$

$$\overline{D}_{xybs} = \left(\left(\frac{1}{12}-\frac{2}{\pi^3}\right)\left(\frac{\nu_{12}\Gamma^4\gamma^2\beta}{1-\nu_{21}\nu_{12}}+\frac{\nu_{21}\Gamma^4\gamma^2}{1-\nu_{21}\nu_{12}}\right)+\frac{\Gamma^4\gamma^2}{1+\nu_{12}}\left(\frac{1}{6}-\frac{4}{\pi^3}\right)+(2\mu^s-\tau^s)\Gamma^4\gamma^2\right),$$
$$\overline{D}_{xyss} = \left(\left(\frac{1}{12}-\frac{4}{\pi^3}+\frac{1}{2\pi^2}\right)\left(\frac{\nu_{12}\Gamma^4\gamma^2\beta}{1-\nu_{21}\nu_{12}}+\frac{\nu_{21}\Gamma^4\gamma^2}{1-\nu_{21}\nu_{12}}\right)+\frac{\Gamma^4\gamma^2}{1+\nu_{12}}\left(\frac{1}{6}-\frac{7}{\pi^3}\right)+\right.$$
$$\left.(2\mu^s-\tau^s)\Gamma^4\gamma^2\right), \quad (A3)$$

$$\overline{D}_{xybgs} = \left(\left(\frac{1}{12}-\frac{2}{\pi^3}\right)\left(\frac{\nu_{12}\Gamma^3\gamma^2\beta}{1-\nu_{21}\nu_{12}}+\frac{\nu_{21}\Gamma^3\gamma^2}{1-\nu_{21}\nu_{12}}\right)+\frac{\Gamma^3\gamma^2}{1+\nu_{12}}\left(\frac{1}{6}-\frac{4}{\pi^3}\right)\right),$$
$$\overline{D}_{xysgs} = \left(\left(\frac{1}{12}-\frac{4}{\pi^3}+\frac{1}{2\pi^2}\right)\left(\frac{\nu_{12}\Gamma^3\gamma^2\beta}{1-\nu_{21}\nu_{12}}+\frac{\nu_{21}\Gamma^3\gamma^2}{1-\nu_{21}\nu_{12}}\right)+\frac{\Gamma^3\gamma^2}{1+\nu_{12}}\left(\frac{1}{6}-\frac{7}{\pi^3}\right)\right), \quad (A4)$$

$$\overline{D}_{ybs} = \left(\left(\frac{1}{12}-\frac{2}{\pi^3}\right)\left(\frac{\Gamma^4\gamma^4\beta}{1-\nu_{21}\nu_{12}}\right)+(2\mu^s+\lambda^s)\Gamma^4\gamma^4\right),$$
$$\overline{D}_{yss} = \left(\left(\frac{1}{12}-\frac{4}{\pi^3}+\frac{1}{2\pi^2}\right)\left(\frac{\Gamma^4\gamma^4\beta}{1-\nu_{21}\nu_{12}}\right)+(2\mu^s+\lambda^s)\Gamma^4\gamma^4\right), \quad (A5)$$

$$\overline{D}_{ygbs} = \left(\frac{1}{12}-\frac{2}{\pi^3}\right)\left(\frac{\Gamma^3\gamma^4\beta}{1-\nu_{21}\nu_{12}}\right),$$
$$\overline{D}_{ygss} = \left(\left(\frac{1}{12}-\frac{4}{\pi^3}+\frac{1}{2\pi^2}\right)\left(\frac{\Gamma^3\gamma^4\beta}{1-\nu_{21}\nu_{12}}\right)\right), \quad (A6)$$

$$\overline{D}_{xbb} = \left(\left(\frac{1}{12}\right)\left(\frac{\Gamma^4}{1-\nu_{21}\nu_{12}}\right)+(2\mu^s+\lambda^s)\Gamma^4\right),$$
$$\overline{D}_{xsb} = \left(\left(\frac{1}{12}-\frac{2}{\pi^3}\right)\left(\frac{\Gamma^4}{1-\nu_{21}\nu_{12}}\right)+(2\mu^s+\lambda^s)\Gamma^4\right), \quad (A7)$$

$$\overline{D}_{xybb} = \left(\left(\left(\frac{1}{12}\right)\left(\frac{\nu_{12}\Gamma^4\gamma^2\beta}{1-\nu_{21}\nu_{12}}+\frac{\nu_{21}\Gamma^4\gamma^2}{1-\nu_{21}\nu_{12}}\right)+(2\mu^s-\tau^s)\Gamma^4\gamma^2\right)+\right.$$
$$\left.\frac{\Gamma^4\gamma^2}{6(1+\nu_{12})}\right)$$
$$\overline{D}_{xysb} = \left(\left(\frac{1}{12}-\frac{2}{\pi^3}\right)\left(\frac{\nu_{12}\Gamma^4\gamma^2\beta}{1-\nu_{21}\nu_{12}}+\frac{\nu_{21}\Gamma^4\gamma^2}{1-\nu_{21}\nu_{12}}\right)+\frac{\Gamma^4\gamma^2}{(1+\nu_{12})}\left(\frac{1}{6}-\frac{4}{\pi^3}\right)+\right.$$
$$\left.(2\mu^s-\tau^s)\Gamma^4\gamma^2\right), \quad (A8)$$

$$\overline{D}_{ybb} = \left(\left(\frac{1}{12}\right)\left(\frac{\Gamma^4\gamma^4\beta}{1-\nu_{21}\nu_{12}}\right)+(2\mu^s+\lambda^s)\Gamma^4\gamma^4\right),$$
$$\overline{D}_{ysb} = \left(\left(\frac{1}{12}-\frac{2}{\pi^3}\right)\left(\frac{\Gamma^4\gamma^4\beta}{1-\nu_{21}\nu_{12}}\right)+(2\mu^s+\lambda^s)\Gamma^4\gamma^4\right), \quad (A9)$$

$$\overline{D}_{xbgb} = \left(\left(\frac{1}{12}\right)\left(\frac{\Gamma^3}{1-\nu_{21}\nu_{12}}\right)\right),$$
$$\overline{D}_{xsgb} = \left(\frac{1}{12}-\frac{2}{\pi^3}\right)\left(\frac{\Gamma^3}{1-\nu_{21}\nu_{12}}\right), \quad (A10)$$

$$\overline{D}_{xybgb} = \left( \left( \left(\frac{1}{12}\right)\left(\frac{\nu_{12}\Gamma^3\gamma^2\beta}{1-\nu_{21}\nu_{12}} + \frac{\nu_{21}\Gamma^3\gamma^2}{1-\nu_{21}\nu_{12}}\right)\right) + \frac{\Gamma^3\gamma^2}{6(1+\nu_{12})} \right),$$

$$D_{xysgb} = \left( \left(\frac{1}{12} - \frac{2}{\pi^3}\right)\left(\frac{\nu_{12}\Gamma^4\gamma^2\beta}{1-\nu_{21}\nu_{12}} + \frac{\nu_{21}\Gamma^4\gamma^2}{1-\nu_{21}\nu_{12}}\right) + \frac{\Gamma^4\gamma^2}{(1+\nu_{12})}\left(\frac{1}{6} - \frac{4}{\pi^3}\right)\right), \tag{A11}$$

$$\overline{D}_{ybgb} = \left( \left(\frac{1}{12}\right)\left(\frac{\Gamma^3\gamma^4\beta}{1-\nu_{21}\nu_{12}}\right)\right)$$
$$\overline{D}_{ysgb} = \left(\frac{1}{12} - \frac{2}{\pi^3}\right)\left(\frac{\Gamma^3\gamma^4\beta}{1-\nu_{21}\nu_{12}}\right), \tag{A12}$$

$$\bar{I}_o = \left(2\rho^s\Gamma + \Gamma^2\right), \tag{A13}$$

$$\bar{I}_{3bs} = \left(\frac{1}{12} - \frac{2}{\pi^3}\right)\lambda^2\Gamma^4(1+\gamma^2),$$
$$\bar{I}_{3ss} = \left(\frac{1}{12} - \frac{4}{\pi^3} + \frac{1}{2\pi^2}\right)\lambda^2\Gamma^4(1+\gamma^2), \tag{A14}$$

$$\bar{I}_{xbs} = \left(-\left(\frac{1}{12} - \frac{2}{\pi^3}\right)\Gamma^4 - 2\rho^s\lambda^2\Gamma - \lambda^2\Gamma^2\right),$$
$$\bar{I}_{xss} = -\left(\Gamma^4\left(\frac{1}{12} - \frac{4}{\pi^3} + \frac{1}{2\pi^2}\right) + 2\rho^s\lambda^2\Gamma + \lambda^2\Gamma^2\right), \tag{A15}$$

$$\bar{I}_{2bs} = \left(\frac{1}{12} - \frac{2}{\pi^3}\right)\lambda^2\Gamma^4,$$
$$\bar{I}_{2ss} = \left(\frac{1}{12} - \frac{4}{\pi^3} + \frac{1}{2\pi^2}\right)\lambda^2\Gamma^4, \tag{A16}$$

$$\bar{I}_{ybs} = \left(-\left(\frac{1}{12} - \frac{2}{\pi^3}\right)\Gamma^4\gamma^2 - \lambda^2\Gamma^2\gamma^2 - 2\rho^s\Gamma\gamma^2\lambda^2\right),$$
$$\bar{I}_{yss} = \left(-\left(\frac{1}{12} - \frac{4}{\pi^3} + \frac{1}{2\pi^2}\right)\Gamma^4\gamma^2 - \lambda^2\Gamma^2\gamma^2 - 2\rho^s\Gamma\gamma^2\lambda^2\right), \tag{A17}$$

$$\bar{I}_{4bs} = \left(\frac{1}{12} - \frac{2}{\pi^3}\right)\lambda^2\Gamma^4\gamma^2,$$
$$\bar{I}_{4ss} = \left(\frac{1}{12} - \frac{4}{\pi^3} + \frac{1}{2\pi^2}\right)\lambda^2\Gamma^4\gamma^2, \tag{A18}$$

$$\bar{I}_{xbb} = -\left(\Gamma^4\left(\frac{1}{12}\right) + 2\rho^s\lambda^2\Gamma\right),$$
$$\bar{I}_{xsb} = \left(-\left(\frac{1}{12} - \frac{2}{\pi^3}\right)\Gamma^4 - 2\rho^s\lambda^2\Gamma\right), \tag{A19}$$

$$\bar{I}_{2bb} = \left(\frac{1}{12}\right)\lambda^2\Gamma^4,$$
$$\bar{I}_{2sb} = \left(\frac{1}{12} - \frac{2}{\pi^3}\right)\lambda^2\Gamma^4, \tag{A20}$$

$$\bar{I}_{3bb} = \left(\frac{1}{12}\right)\lambda^2\Gamma^4(1+\gamma^2),$$
$$\bar{I}_{3sb} = \left(\frac{1}{12} - \frac{2}{\pi^3}\right)\lambda^2\Gamma^4(1+\gamma^2), \tag{A21}$$

$$\bar{I}_{ybb} = \left(-\left(\frac{1}{12}\right)\Gamma^4\gamma^2 - \lambda^2\Gamma^2\gamma^2 - 2\rho^s\Gamma\lambda^2\right),$$
$$\bar{I}_{ysb} = \left(-\left(\frac{1}{12} - \frac{2}{\pi^3}\right)\Gamma^4\gamma^2 - \lambda^2\Gamma^2\gamma^2 - 2\rho^s\Gamma\lambda^2\right), \tag{A22}$$

$$\bar{I}_{4bb} = \left(\frac{1}{12}\right)\lambda^2\Gamma^4\gamma^2,$$
$$\bar{I}_{4sb} = \left(\frac{1}{12} - \frac{2}{\pi^3}\right)\lambda^2\Gamma^4\gamma^2, \tag{A23}$$

## References


[1] H.C. Nathanson, W.E. Newell, R.A. Wickstrom, J.R. Davis, The resonant gate transistor, IEEE Trans. Electron Devices 117 (1967) 133.
[2] H.A.C. Tilmans, R. Legtenberg, Electrostatically driven vacuum-encapsulated polysilicon resonators part II. Theory and performance, Sensors Actuators A (1994) 67–84.
[3] P.M. Osterberg, S.D. Senturia, M-TEST: a test chip for MEMS material property measurement using electrostatically actuated test structures, J. Microelectromech. Syst. (1997) 107–118.
[4] G. Li, N.R. Alura, A Lagrangian approach for quantum-mechanical electrostatic analysis of deformable silicon nanostructures, Eng. Bound. Elem. (2006) 925–932.
[5] S.K. Lamoreaux, The Casimir force: background, experiments, and applications, Rep. Prog. Phys. (2005) 201–236.
[6] M. Dequesnes, S.V. Rotkin, N.R. Aluru, Calculation of pull-involtages for carbonnanotube-based nanoelectromechanical switches, Nanotechnology (2002) 120–131.
[7] M. Janghorban, Static and free vibration analysis of carbon nano-wires based on Timoshenko beam theory using differential quadrature method, Lat. Am. J. Solids Struct. (2011) 463–472.
[8] J.G. Guo, Y.P. Zhao, Dynamic stability of electrostatic torsional actuators with van der Waals effect, Int. J. Solids Struct. (2006) 675–685.
[9] Y. Chan, N. Thamwattana, J.M. Hill, Axial buckling of multiwalled carbon nanotubes and nanopeapods, Eur. J. Mech. A. Solids (2011) 794–806.
[10] A. Koochi, A. Noghrehabadi, M. Abadyan, Approximating the effect of van der Waals force on the instability of electrostatic nano-cantilevers, Int. J. Mod. Phys. B (2011) 3965–3976.
[11] KoochiA SoroushR, A.S. Kazemi, M. Abadyan, Modeling the effect of van der Waals attraction on the instability cantilever and doubly- of electrostatic supported nano-beams using modified adomian method, Int. J. Struct. Stab. Dyn. (2012) 1250036–1250046.
[12] A. Ramezani, A. Alasty, J. Akbari, Closed-formsolutions of the pull-in n instability in nano-cantilevers under electrostatic and intermolecular surface forces, Int. J. Solids Struct. (2007) 4925–4941.
[13] N. Taghavi, H. Nahvi, Pull-in instability of cantilever and fixedefixed nano-switches, Eur. J. Mech. A. Solids (2013) 123–133.
[14] R.C. Batra, M. Porfiri, D. Spinello, Vibrations and pull-in instabilities of microelectromechanical von Karman elliptic plates incorporating the Casimir force, J. Sound Vib. 315 (2008) 939–960.
[15] W.H. Lin, Y.P. Zhao, Dynamic behavior of nanoscale electrostatic actuators, Chin. Phys. Lett. 20 (2003) 2070–2073.
[16] L.J. Xiao, J. Yang, S. Kitipornchai, Pull-in instability of geometrically nonlinear micro-switches under electrostatic and Casimir forces, Acta Mech. 218 (2011) 161–174.
[17] E.M. Abdel Rahman, M.I. Younis, A.H. Nayfeh, Characterization of the mechanical behavior of an electrically actuated microbeam, J. Micromech. Microeng. (2002) 759–766.
[18] J.H. Kuang, C.J. Chen, Dynamic characteristics of shaped micro-actuators solvedusing the differential quadrature method, J. Micromech. Microeng. (2004) 647–655.
[19] H.A.C. Tilmans, R. Legtenberg, Electrostatically driven vacuum-encapsulated polysilicon resonators, part II: theory and performance, Sensors Actuators A Phys. (1994) 67–84.
[20] E.S. Hung, S.D. Senturia, Extending the travelrange of analog-tuned electrostatic actuators, J. Microelectron. Syst. (1999) 497–505.
[21] R. Javaheri, M.R. Eslami, Buckling of functionally graded plates under in-plane compressive loading, J. Appl. Math. Mech. (2002) 277–283.
[22] D.G. Zhang, Y.H. Zhou, A theoretical analysis of FGM thin plates based on physical neutral surface, Comput. Mater. Sci. (2008) 716–720.
[23] SaidiAR MohammadiM, E. Jomehzadeh, Levy solution for buckling analysis of functionally graded rectangular plates, Appl. Compos. Mater. (2010) 81–93.
[24] SaidiAR BodaghiM, Stability analysis of functionally graded rectangular plates under nonlinearly varying in-plane loading resting on elastic foundation, Arch. Appl. Mech. (2011) 765–780.
[25] A.C. Eringen, On differential equations of nonlocal elasticity and solutions of screw dislocation and surface waves, J. Appl. Phys. (1993) 4703–4710.
[26] A.C. Eringen, D.G.B. Edelen, On nonlocal elasticity, Int. J. Eng. Sci. 10 (1972) 233–248.
[27] J. Yang, X.L. Jia, S. Kitipornchai, Pull-in instability of nano-switches using nonlocal elasticity theory, J. Phys. D. Appl. Phys. 41 (2008) 035103.
[28] A. Ghorbanpour Arani, M. Ghaffari, A. Jalilvand, R. Kolahchi, Nonlinear nonlocal pull-in instability of boron nitride nanoswitches, Acta Mech. 3005 (2013) 3019.
[29] Y. Su, H. Wei, R. Gao, Z. Yang, J. Zhang, Z. Zhong, Exceptional negative thermal expansion and viscoelastic properties of graphene oxide paper, Carbon (2012) 2804–2809.
[30] J. Zhang, Fu Yiming, Pull-in analysis of electrically actuated viscoelastic microbeams based on a modified couple stress theory, Meccanica 47 (2012) 1649–1658.
[31] H.M. Ma, X.L. Gao, J.N. Reddy, A microstructuredependent Timoshenko beam model based on a modified couple stress theory, J. Mech. Phys. Solids (2008) 3379–3391.
[32] K.F. Wang, B.L. Wang, Influence of surface energy on the non-linear pull-in instability of nano-switches, Int. J. Non Linear Mech. (2014) 69–75.
[33] S. Basu, A. Prabhakar, E. Bhattacharya, Estimation of stiction force from electrical and optical measurements on cantilever beams, J. Microelectromech. Syst. 16 (2007) 1254–1262.
[34] S. Chakraborty, A. Bhattacharya, T.K. Bhattacharyya, Experimental analysis of pull-out voltage of electrostatically actuated microcantilever beam based on contact-stiction model, Micro Nano Lett. 6 (2011) 43–47.

[35] Tong Qing Lu, Wei Xu Zhang, T.J. Wang, The surface effect on the strain energy release rate of buckling delamination in thin film–substrate systems, Int. J. Eng. Sci. (2011) 967–975.
[36] M.E. Gurtin, A.I. Murdoch, A continuum theory of elastic material surface, Arch. Ration. Mech. Anal. 57 (1975) 291–323.
[37] M.T. SakhaeePour, M.T. Ahmadian, A. Vafai, Applications of single-layered graphene sheets as mass sensors and atomistic dust detectors, Solid State Commun. 145 (2008) 168–172.
[38] Huu Tai Thai, P.V.O. Thuc, A new sinusoidal shear deformation theory for bending, buckling, and vibration of functionally graded plates, Appl. Math. Model. (2013) 3269–3281.
[39] S. Pouresmaeeli, E. Ghavanloo, S.A. Fazelzadeh, Vibration analysis of viscoelastic orthotropic nano-plates resting on viscoelastic medium, Compos. Struct. (2013) 405–410.
[40] M.I. Younis, Abdel-RahmanEM NayfehAH, Reduced-order models for MEMS applications, Nonlinear Dyn. (2005) 211–236.
[41] S.S. Rao, Mechanical Vibrations, fourth ed. Pearson, Prentice-Hall, Englewood Cliffs, NJ, 2004.
[42] T. Mousavi, S. Bornassi, H. Haddadpour, The effect of small scale on the pull-in instability of nano-switches using DQM, Int. J. Solids Struct. 50 (2013) 1193–1202.